Impact of urbanization on US surface climate

You may also be interested in:

Interactions between urban vegetation and surface urban heat islands: a case study in the Boston metropolitan region
Eli K Melaas, Jonathan A Wang, David L Miller et al.

Investigating the climate impacts of urbanization and the potential for cool roofs to counter future climate change in Southern California
P Vahmani, F Sun, A Hall et al.

Climate–vegetation control on the diurnal and seasonal variations of surface urban heat islands in China
Decheng Zhou, Liangxia Zhang, Dan Li et al.

Quality and sensitivity of high-resolution numerical simulation of urban heat islands
Dan Li and Elie Bou-Zeid

Contrasting responses of urban and rural surface energy budgets to heat waves explain synergies between urban heat islands and heat waves
Dan Li, Ting Sun, Maofeng Liu et al.

A global map of urban extent from nightlights
Yuyu Zhou, Steven J Smith, Kaiguang Zhao et al.

Towards typologies of urban climate and global environmental change
Felix Creutzig

Contrasting impacts of urban forms on the future thermal environment: example of Beijing metropolitan area
Long Yang, Dev Niyogi, Mukul Tewari et al.

Environmental Research Letters

Impact of urbanization on US surface climate

Lahouari Bounoua[1], Ping Zhang[1,2,8], Georgy Mostovoy[2,1], Kurtis Thome[1], Jeffrey Masek[1], Marc Imhoff[2], Marshall Shepherd[3], Dale Quattrochi[4], Joseph Santanello[5], Julie Silva[6], Robert Wolfe[7] and Ally Mounirou Toure[8,1]

[1] Biospheric Sciences Laboratory, NASA's Goddard Space Flight Center, Greenbelt, MD, USA
[2] Earth System Science Interdisciplinary Center, University of Maryland, College Park, MD, USA
[3] Department of Geography, University of Georgia, Athens, GA, USA
[4] Marshal Space Flight Center, MSFC, Huntsville, AL, USA
[5] Hydrological Sciences Laboratory, NASA's Goddard Space Flight Center, Greenbelt, MD, USA
[6] Department of Geographical Sciences, University of Maryland College Park, 2181 LeFrak Hall, College Park, MD, USA
[7] Terrestrial Information Systems Laboratory, NASA's Goddard Space Flight Center, Greenbelt, MD, USA
[8] Science System Applications Inc., Lanham, MD, USA

E-mail: Lahouari.Bounoua@nasa.gov

Abstract

We combine Landsat and MODIS data in a land model to assess the impact of urbanization on US surface climate. For cities built within forests, daytime urban land surface temperature (LST) is much higher than that of vegetated lands. For example, in Washington DC and Atlanta, daytime mean temperature differences between impervious and vegetated lands reach 3.3 and 2.0 °C, respectively. Conversely, for cities built within arid lands, such as Phoenix, urban areas are 2.2 °C cooler than surrounding shrubs. We find that the choice and amount of tree species in urban settings play a commanding role in modulating cities' LST. At continental and monthly scales, impervious surfaces are 1.9 °C ± 0.6 °C warmer than surroundings during summer and expel 12% of incoming precipitation as surface runoff compared to 3.2% over vegetation. We also show that the carbon lost to urbanization represents 1.8% of the continental total, a striking number considering urbanization occupies only 1.1% of the US land. With a small areal extent, urbanization has significant effects on surface energy, water and carbon budgets and reveals an uneven impact on surface climate that should inform upon policy options for improving urban growth including heat mitigation and carbon sequestration.

1. Introduction

Viewed from the perspective of the amount of space it currently occupies, urbanization appears as a minor form of land transformation. However, in terms of ecological impact it is one of the most significant and long lasting forms of land transformation and its extent of increase is at least proportional to population growth and economic development (Shepherd *et al* 2013). The cumulative signature of this anthropogenic land cover (LC) disturbance is reaching higher proportions in some regions of the world and may already be playing a role in local and regional scale biological, hydrological, energetic and socio-economic activities (e.g., Güneralp and Seto 2013,

Mahmood *et al* 2014, McDonald *et al* 2014). Given these seemingly conflicting attributes of small area but high ecological impact of urbanization and its expected increase, it is important to assess its rate of change and its impacts on the biological, hydrological and energy cycles for the continental USA.

Urbanization affects its environment through several distinct but coupled mechanisms: the first and most significant impact is expressed by the reduction of the fraction of vegetation (e.g., Bounoua *et al* 2009, Qureshi *et al* 2010) and the subsequent inhibition of photosynthetic activity and plant's water transpiration and interception losses. The second impact comes from the introduction in the landscape of an impervious surface (IS) which alters the partitioning of

surface runoff and water infiltration into the ground, and modifies the soil moisture content and water table. The third impact results from changes in surface albedo (e.g., Akbari 2002) and its effect on the surface energy partitioning; while the fourth impact is associated with a modification of the surface roughness and its implication for the surface turbulent fluxes and diffusion of heat (e.g., Zhao *et al* 2014, Oke 1988).

Urbanization is often concentrated to specific areas within landscape and forms heterogeneous patches with respect to surface radiation and other elements of the energy, water and carbon budgets. Therefore it needs to be studied at spatial and temporal scales fine enough to capture the responses of different LC elements existing within and immediately surrounding the build-up. At the local scale, case studies have illustrated its effects on surface temperature and hydrology (Shepherd 2006, Bounoua *et al* 2009, Sajjad *et al* 2009). Over larger scales however, little (e.g.; Oleson *et al* 2013) has been done to quantify its aggregate impact due in part to lack of LC data at space and time scales appropriate for resolving the urban metabolism within larger scale climate. Landsat data have a fine spatial resolution (30 m) from which impervious surface area (ISA) can be estimated at continental scale and, combined with the Moderate Resolution Imaging Spectroradiometer (MODIS) products to describe the phenology of the surrounding vegetated lands, provide a unique characterization of the urban environment.
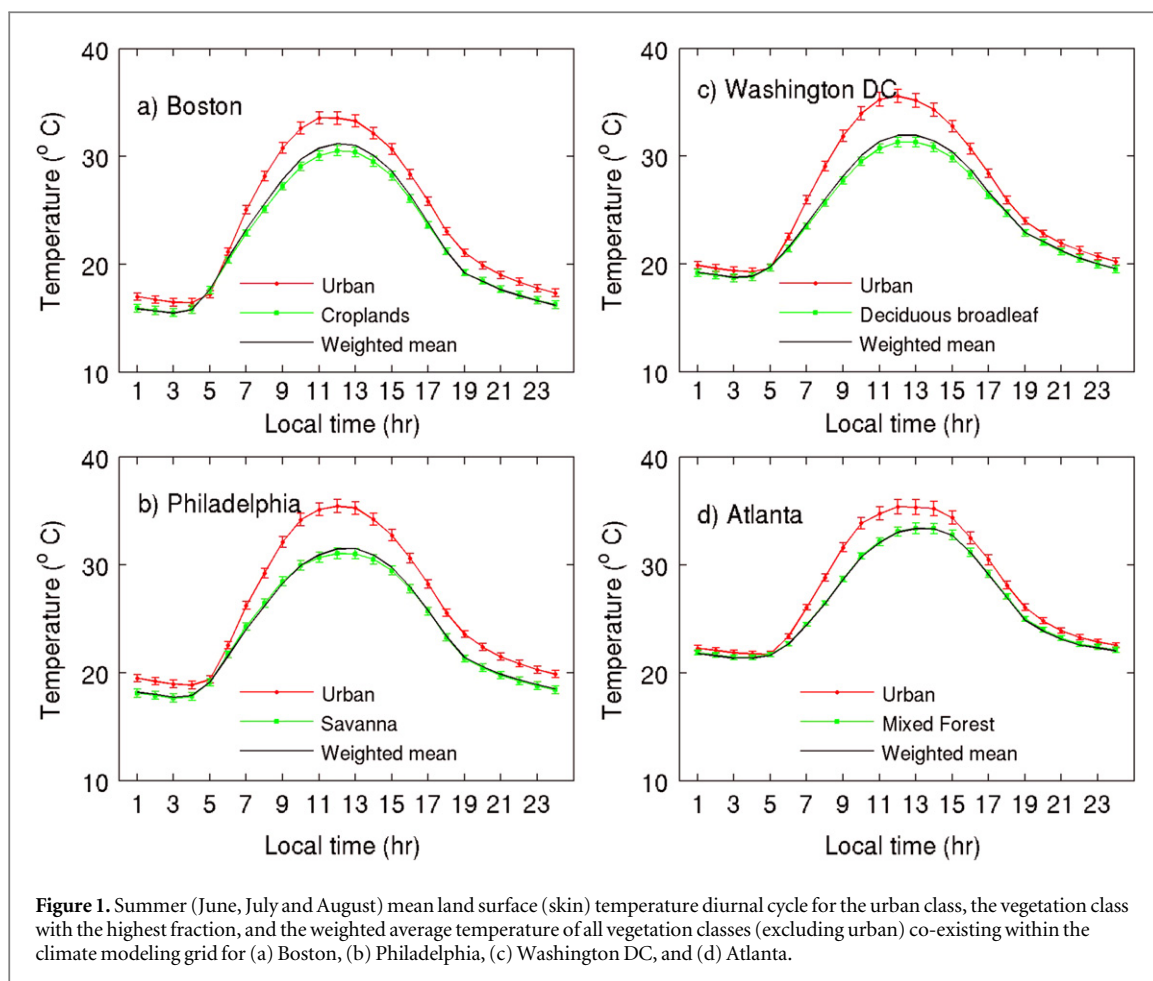
While most previous studies evaluating the urban heat island (UHI) at the US continental scale have consisted of static, remote sensing-based analysis of the UHI amplitude (e.g., Imhoff *et al* 2010, Zhang *et al* 2010), in this paper we use a fusion of Landsat and MODIS data in the Simple Biosphere model (SiB2) of Sellers *et al* (1996a) as modified by Bounoua *et al* (2009) to describe the UHI and its amplitude and evolution at different time and space scales. Specifically, we use the Landsat-based ISA from the National Land Cover Dataset (NLCD) (Homer *et al* 2004) to characterize the urban areas at 30 m × 30 m spatial resolution, and MODIS-based biophysical products at 500 m × 500 m spatial resolution and 8-day time-interval to describe the vegetation phenology within a climate modeling grid (CMG) of 0.05° × 0.05° of latitude–longitude (approximately 5 km × 5 km) over the continental United States (CONUS) to simulate the impact of urbanization as a form of land use on the surface energy, carbon and water cycles for 2001.

2. Method

Landsat-based ISA from the NLCD was used to characterize urban LC at 30 m spatial resolution over the CONUS for 2001 (Homer *et al* 2004). The ISA data was combined with MODIS LC at 500 m spatial resolution and then aggregated into a 5 km × 5 km CMG. This data fusion considers ISA as a reliable product to characterize the build-up and was implemented as follows: (1) we co-registered the Landsat data to the CMG and aggregated the ISA from 30 m to 5 km × 5 km resolution, (2) we aggregated the different cover types from the 500m MODIS LC map (MCD12Q1) and obtained fractions in the CMG, (3) we then imposed the aggregated ISA fractions into the CMG in lieu of the MODIS build-up. When imposing Landsat-based ISA into the CMG, differences between ISA fractions and MODIS build-up fractions were proportionally distributed over other non-impervious LC types co-existing in the CMG. The distribution was weighted by fractions of LC types existing in the CMG. Each CMG may have up to 12 LC classes with their fractions within the CMG obtained from higher resolution Landsat and MODIS data (Bounoua *et al* 2015). For each LC class in the CMG a set of biophysical parameters was generated at the same resolution using the 8-day composite 500m gap-filled North American Carbon Program MODIS normalized difference vegetation index (Tan *et al* 2011, Bounoua *et al* 2015). Along with other vegetation physiological, optical and morphological parameters, these biophysical parameters served as surface boundary conditions to SiB2. Urban IS is characterized with a heat absorption function represented by an average heat capacity of a thin concrete slab modulated by diurnally varying sun angle, and augmented by the heat capacity of water and snow on the ground.

The SiB2 model is driven by external meteorological data in an offline mode over the CONUS. The initialization is done iteratively using the fraction of photosynthetically active radiation based on the logic that vegetation density is in quasi-equilibrium with climate and the amount of soil water (Stefanova 2001). The model was spun up for 5 years forced by hourly meteorological data at 5 km × 5 km obtained from the North American Land Data Assimilation System NLDAS-2, interpolated using a Lagrangian interpolation in time from hourly to half-hourly and a bi-linear interpolation in space from 0.125° × 0.125° to 0.05° × 0.05° grid spacing. The model was integrated independently for each of the twelve LC classes and outputs from different integrations are stratified by LC, as well as a weighted average obtained as a response from each LC weighted by its fraction within the CMG. The simulations differ in their LC types, morphological, optical and physiological attributes, and the associated vegetation phenological parameters derived from MODIS. Each simulation was integrated forward another 3 years after spin up using the same atmospheric drivers so that model responses are exclusively attributable to changes in LC. The simulations do not account for feedback to the atmosphere and therefore allows us to isolate the effects of landscape differences on local to continental scale near-surface climate conditions. In this analysis, we present

Figure 1. Summer (June, July and August) mean land surface (skin) temperature diurnal cycle for the urban class, the vegetation class with the highest fraction, and the weighted average temperature of all vegetation classes (excluding urban) co-existing within the climate modeling grid for (a) Boston, (b) Philadelphia, (c) Washington DC, and (d) Atlanta.

results from model outputs averaged over the last three years of model integration.

3. Results and discussion

Hourly outputs were saved, for an *a priori* selection of 90 CMGs and for the entire year; 24 of these CMGs are within cities selected to spatially represent major ecoregions of the CONUS and have the highest ISA fraction. CMGs belonging to the same ecoregion exhibited a similar surface temperature diurnal evolution with some variations in the maximum temperature. We therefore limited our discussion on the surface temperature to 10 cities. In this study we report about the surface urban heat island (SUHI) defined as difference in land surface temperature (LST) between the ISA and the vegetated land surrounding it, which is different from the classical UHI based on air temperature. Summer mean LST diurnal cycles are shown for select CMGs in US cities. Each CMG contains multiple LC types; however, only three temperature profiles are displayed: (1) the IS class, (2) the vegetation class with the highest fraction, and (3) the weighted average from vegetation classes only (excluding urban).

For the Eastern US cities (figure 1), the urban daytime mean LST is much higher than that of the vegetated class, with differences reaching 2.0 °C in Atlanta

and 3.3 °C in Washington DC For these cities, the absolute maximum temperature differences between urban and vegetated lands are 3.1 and 4.5 °C, respectively and occur in the morning (11:00 AM) when the urban class warms faster than vegetation. For all cities, the vegetation's temperature presents a noticeable diurnal asymmetry during afternoons when solar radiation is maximal. Vegetation temperature is largely determined by local weather; however the extent of its diurnal variation is modulated by the plant's physiological activity. To regulate the capture of CO_2 from the atmosphere and the simultaneous diffusion of water from the leaf interior, plants close their stomata during high irradiance, shunting most of the absorbed energy into sensible heating, thus increasing vegetation temperature during afternoons as compared to mornings. For example, in Atlanta GA, this asymmetry is characterized by an LST difference between the impervious and vegetated LC of 3.0 °C at 9:00 AM (ΔT_{am}) and 1.6 °C at 3:00 PM (ΔT_{pm}). The difference between ΔT_{am} and ΔT_{pm} is attenuated as surface temperature decreases with latitude. Indeed, in Boston ΔT_{am} is 2.9 °C and ΔT_{pm} is 2.0 °C (figure 1).

The composition and vegetation fractional coverage within landscapes play an important role in the city's energy budget. In Washington DC, composed of approximately 52% IS, 24% broadleaf deciduous (BD)
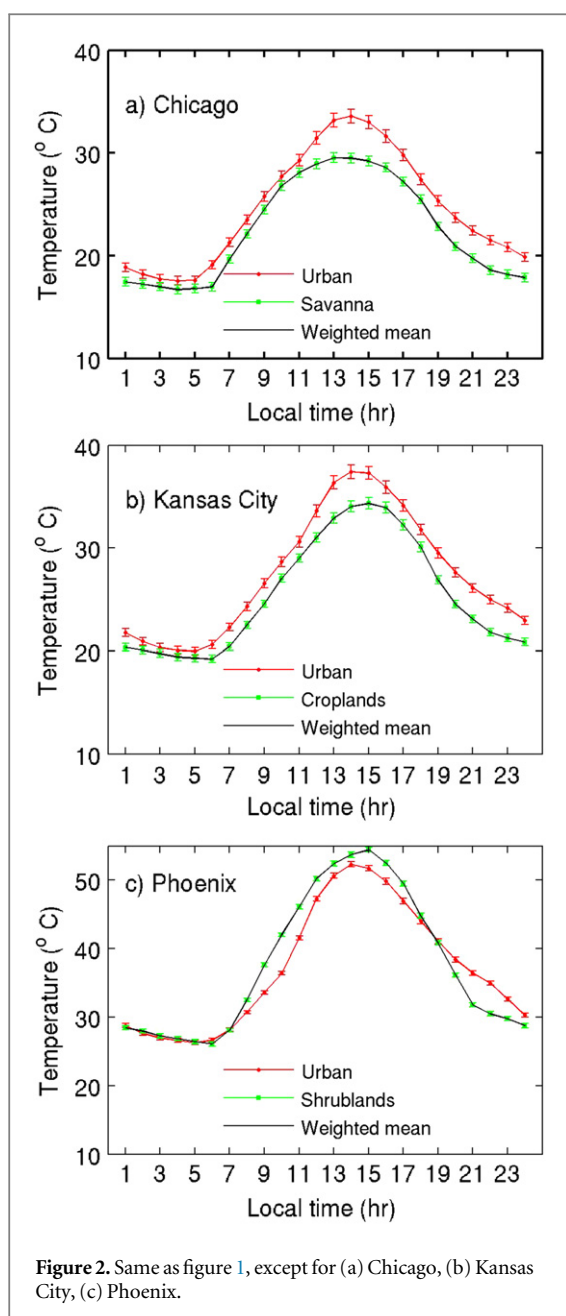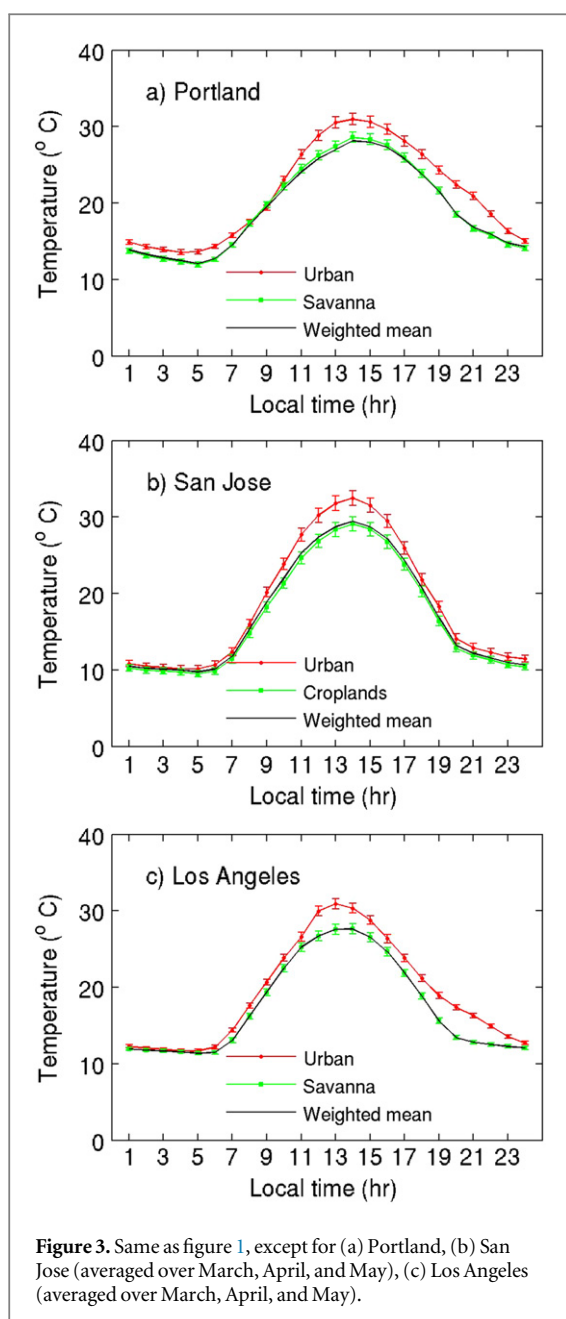
Figure 2. Same as figure 1, except for (a) Chicago, (b) Kansas City, (c) Phoenix.

and 24% mixed forest (MF), the daytime mean surface temperature difference between impervious and forested areas varies between 2.4 °C for the MF to 3.3 °C for the BD. This result, partly due to the fact that BD trees are more heat tolerant than the MF, suggests that the choice of a mix of trees within an urban composition is an important ecosystem service in the regulation of surface temperature and the SUHI mitigation. Our results also indicate that nighttime temperature differences between IS and surrounding vegetation is larger for those parts of cities built within short (savanna-type and cropland) vegetation such as the points in Boston MA and Philadelphia PA (figures 1(a) and (b)) than those built within tall trees such as Atlanta and Washington DC (figures 1(c) and (d)). For cities built in a temperate grassland/C3 agriculture biome such as Chicago IL with about 72% IS and 28% grassland/

agriculture (figure 2(a)) and Kansas City MO with about 62% IS and 38% croplands (figure 2(b)), the daytime mean temperature difference between the IS and vegetated land is 2.3 and 2.2 °C, respectively. These differences are slightly lower than those simulated in eastern US cities built in forested lands but similar to differences of 2.2 °C obtained for the Boston CMG surrounded by short vegetation. Further south in Phoenix AZ built in a desert, the model simulates temperature within urban areas 2.2 °C cooler than the surrounding desert-like shrublands during daytime but 1.3 °C warmer during nighttime (figure 2(c)) due to introduction of irrigated exotic trees and lawns. The desert shrublands cool faster than urban areas after sunset resulting in urban nighttime temperature warmer than surroundings. These results are in agreement with previous studies (Grimmond *et al* 2002, Pearlmutter *et al* 2007, Imhoff *et al* 2010). In Portland OR, a northwestern city embedded in temperate coniferous forests (figure 3(a)), the daytime mean LST difference between impervious and forested lands is 1.7 °C, slightly less than that simulated for eastern cities built in MFs such as Washington DC and Atlanta, but larger at night when it reaches about 2.0 °C. In San Jose CA and Los Angeles CA (figures 3(b) and (c)) the urban is warmer than vegetation during daytime by 2.4 and 1.9 °C, respectively. Our results are consistent with recent analyses of the relationship between urban intensity and phenology across a region with broadly similar environmental characteristics (Walker *et al* 2015).

In most US cities, the material used in buildings and pavement construction absorbs more energy causing urban surfaces and the air immediately around them to warm faster than surrounding vegetated areas, creating an UHI (Voogt and Oke 2003, Shepherd 2006, Quattrochi *et al* 2007, Imhoff *et al* 2010, Stone *et al* 2013). As reported in Quattrochi *et al* (1997) the SiB2 model reproduces distinct responses from different LC elements forced by the same atmospheric variables, and captures the UHI with results in agreement with observations (Oke 1982, Imhoff *et al* 2010, Zhang *et al* 2010) and modeling studies (Shepherd 2006).

Except for Phoenix AZ where the model simulated an urban heat sink (figure 2(c)), for all other cities, the modeled urban surface temperature is warmer than that of the surrounding vegetated land (figures 1–3), creating thus well-defined UHIs. To illustrate this effect, we choose 2 large cities in close proximity, in the eastern US (Washington DC and Baltimore MD), forming a metropolis of the region, to assess the surface temperature contrast between the urban and vegetated lands. We also compare the UHI of this metropolis with that simulated in a city of similar size in the mid-Atlantic region with warmer climate (Atlanta, GA). We selected an area of about 1.5° × 1.5° of latitude–longitude including Washington DC and Baltimore to illustrate the amplitude and structure of

Figure 3. Same as figure 1, except for (a) Portland, (b) San Jose (averaged over March, April, and May), (c) Los Angeles (averaged over March, April, and May).

the UHI. We analyzed the June–July–August (JJA) surface temperature difference between the impervious class and the weighted average temperature for vegetated classes for each CMG within the area (figure 4). We find temperature differences of more than 2 °C simulated along the northeastern corridor; and in regions with high ISA west of the cities. For Atlanta (not shown), most CMGs (52%) display an urban minus vegetation temperature differences less than 1.7 °C, whereas 53% of CMGs along the Washington-Baltimore corridor show temperature differences greater than 2 °C. This is due to higher summer temperature in Atlanta compared to the Washington DC-Baltimore region, which forces vegetation stomatal closure and increases its canopy temperature, thus reducing its difference from that in urban areas. We represent the UHI using surface

temperature profiles in Washington DC and Baltimore over an area spanning about 75 km around Washington DC city center for: (1) a fully urban scenario (100% IS), (2) a weighted average scenario representing the actual condition and comprising all classes (including IS) weighted by their fractions, and (3) a fully vegetated scenario in which IS is replaced by a weighted mix of vegetation (figure 5). In line with observations (Imhoff *et al* 2010, Zhang *et al* 2010, 2012) and the work of Stone *et al* (2013), simulated results show that surface temperature in city cores is influenced by the IS fraction, and the amplitude of the UHI depends on surrounding LC composition. For example in Baltimore, where ambient air temperature is close to that of Washington DC and where 71.5% (20% more than Washington DC) of the area is impervious, the weighted average surface temperature in the city center is about 0.7 °C warmer than in Washington DC Furthermore, in Baltimore, the UHI amplitude decreases sharply, 1.35 °C, in a short distance (~10 km) away from the city center, due to its LC composition and proximity to water.

The fully vegetated scenario is a proxy for a pre-urban condition, and the departure of its temperature from the weighted average (actual condition) represents the cumulative impact of urbanization on the city's temperature. Using this comparison, we found that urbanization has increased the urban core surface temperature by about 0.9 °C in both Washington DC and Baltimore. Furthermore, if the area were to be fully urbanized, the surface temperature could rise by up to 1.8 °C at the fringes of both cities, while their city centers could warm up another 0.8 and 1.2 °C, respectively. Shepherd *et al* (2013) discussed the concept of how fragmented urban archipelagos scale up to impact climate, and this analysis confirms their theoretical framework. At the continental and monthly scales, spatially averaged over all pixels having more than 1% IS, we find urban lands warmer than their surroundings by 1.9 °C ± 0.6 °C during summer and 1.5 °C ± 0.4 °C during winter. These figures are in agreement with satellite estimated global average summer and winter UHI of 2.6 and 1.4 °C, respectively (Zhang *et al* 2010). This suggests that with increases in worldwide temperatures associated with global warming, cities may experience higher temperatures sooner than expected and the global average 2 °C upper limit endorsed by the United Nations Framework Convention on Climate Change may need to be revised for cities, which will host about 50% of the total population by 2050 (UNFPA 2007). Furthermore, our results indicate that the SUHI is quasi-insensitive to ISA fraction smaller than 35% and increases linearly after that (figure 6) which suggests that small cities, occupying about one third (35%) of their environment, may generate less heat.

We find the daytime mean temperature difference between impervious and vegetated lands to be robustly correlated to daytime accumulated transpiration from
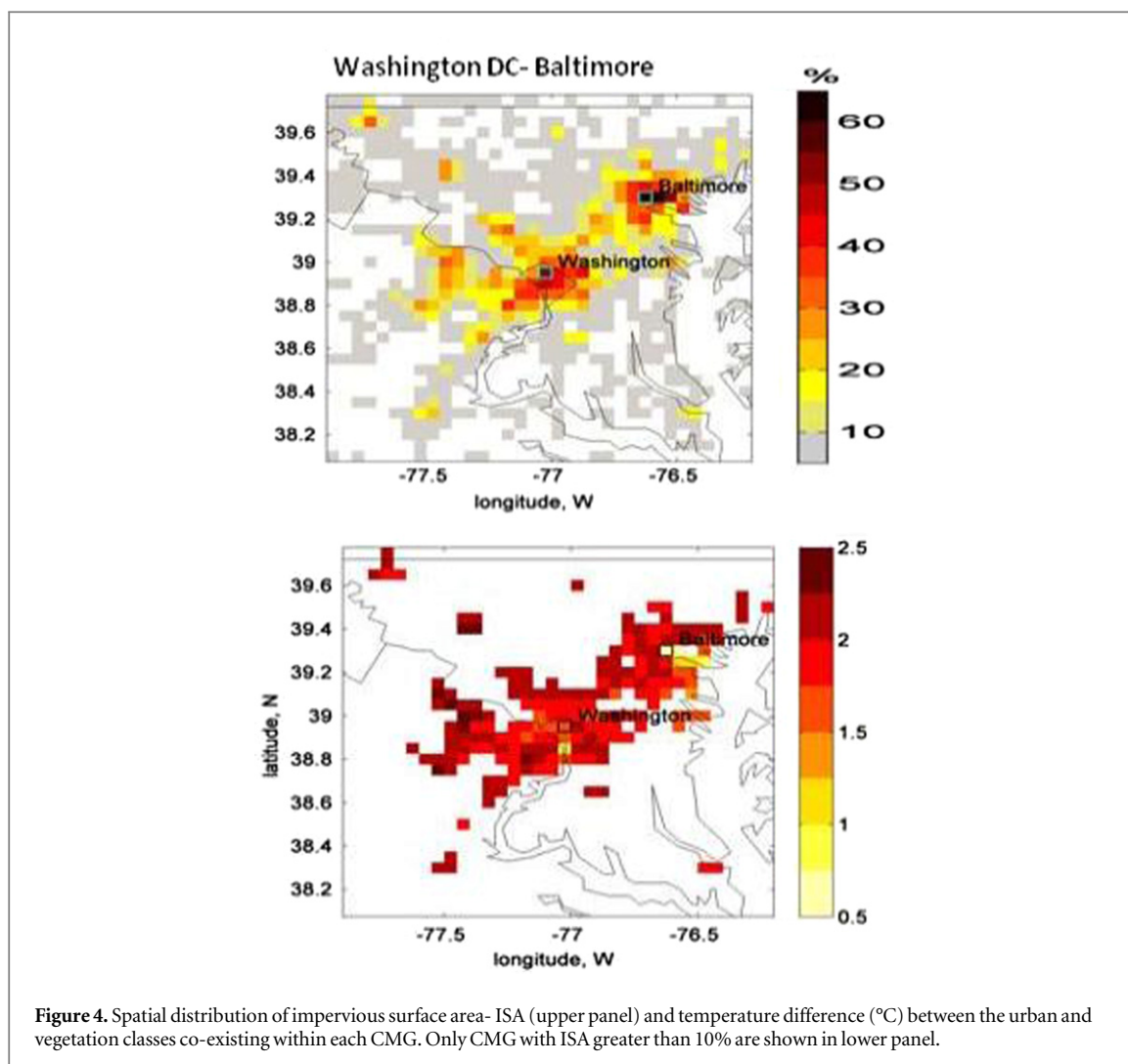
Figure 4. Spatial distribution of impervious surface area- ISA (upper panel) and temperature difference (°C) between the urban and vegetation classes co-existing within each CMG. Only CMG with ISA greater than 10% are shown in lower panel.

vegetation ($R^2 = 0.83$). This suggests that the choice and amount of tree species in urban settings can play a commanding role in modulating cities' overall surface temperature and can be used as a potential 'cooling' mechanism to alleviate the excess warming generated by IS, and to reduce domestic energy consumption. This result is in line with those from Gober *et al* (2009) and complements the quantitative attribution of the various contributions to UHI expressed in Zhao *et al* (2014); it indicates that a large part of the contrast in temperature making the SUHI is generated by evaporative cooling of vegetation surrounding urban areas (figure 7).

The hydrological module of SiB2 distributes the precipitation into canopy interception and throughfall components. Water intercepted by the canopy either evaporates at the potential rate or contributes to throughfall when the canopy holding capacity is exceeded. The combined canopy water is added to the ground liquid water store from which it either evaporates or infiltrates into a shallow surface layer if the ground storage capacity is reached. In SiB2 the IS layer has a variable water storage capacity capped at 2 mm depth, an empirically determined value that matches

modeled results with observations (e.g. Colello *et al* 1998, Ramamurthy and Bou-Zeid 2014). The surface layer has 2 cm depth for all other LC classes (Sellers *et al* 1996b). If the water infiltration rate is higher than the soil infiltration capacity, the excess water contributes to surface runoff.

For the grid cell located in Atlanta, we found that if the entire CMG were impervious, 47% of the precipitation will be expelled as surface runoff during summer (JJA) versus only 3.1% if the entire CMG were MF (table 1). Similar results are obtained for Washington DC with more surface runoff generated by broadleaf trees (BD) dominating the city. Given the satellite measured LC composition, we estimate the annual surface runoff in Atlanta to be about 28.9% of incoming precipitation in the urban area and only about 1.6% over the MF, whereas in Washington DC, it is about 25.7% in the urban area and 2.4% over the BD trees. Considering precipitation is uniformly distributed over the 5 km × 5 km CMG; this ratio is informative about the effect of LC on surface runoff and can be used for projecting the distribution of surface runoff given a rainfall prediction event and for defining the urban storm water guidelines. This ratio may also
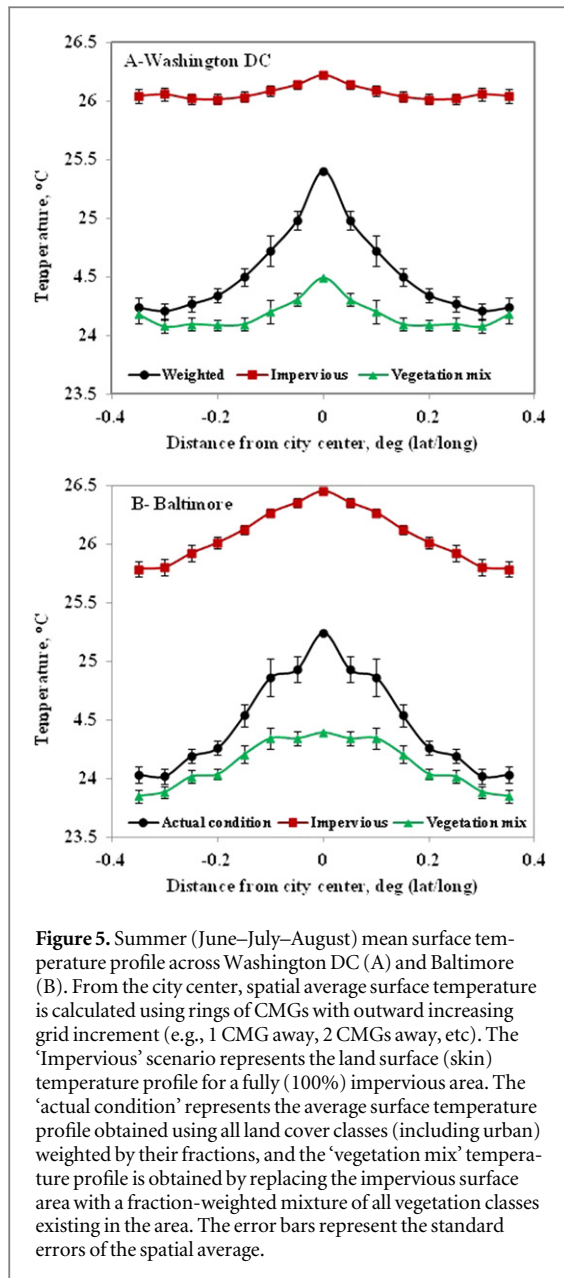
Figure 5. Summer (June–July–August) mean surface temperature profile across Washington DC (A) and Baltimore (B). From the city center, spatial average surface temperature is calculated using rings of CMGs with outward increasing grid increment (e.g., 1 CMG away, 2 CMGs away, etc). The 'Impervious' scenario represents the land surface (skin) temperature profile for a fully (100%) impervious area. The 'actual condition' represents the average surface temperature profile obtained using all land cover classes (including urban) weighted by their fractions, and the 'vegetation mix' temperature profile is obtained by replacing the impervious surface area with a fraction-weighted mixture of all vegetation classes existing in the area. The error bars represent the standard errors of the spatial average.
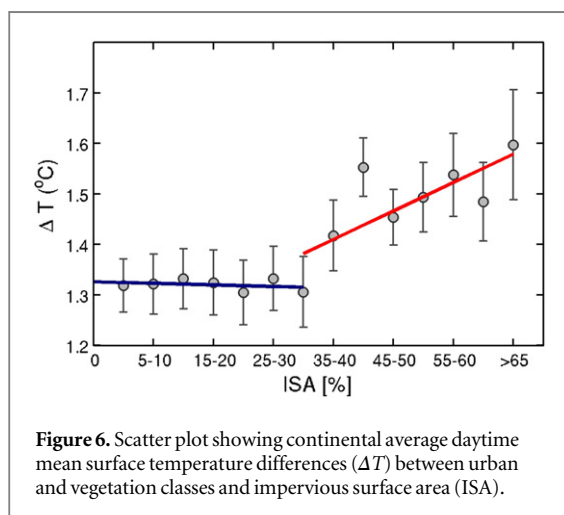

Figure 6. Scatter plot showing continental average daytime mean surface temperature differences (ΔT) between urban and vegetation classes and impervious surface area (ISA).
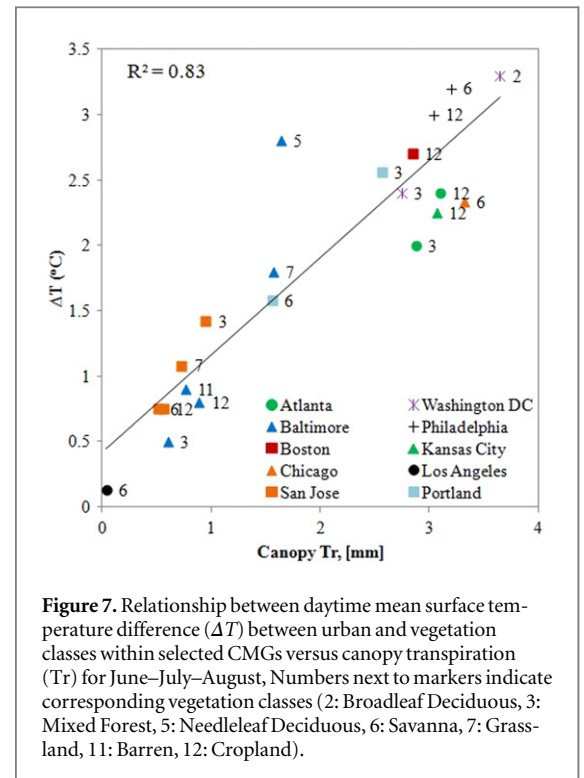

Figure 7. Relationship between daytime mean surface temperature difference (ΔT) between urban and vegetation classes within selected CMGs versus canopy transpiration (Tr) for June–July–August, Numbers next to markers indicate corresponding vegetation classes (2: Broadleaf Deciduous, 3: Mixed Forest, 5: Needleleaf Deciduous, 6: Savanna, 7: Grassland, 11: Barren, 12: Cropland).

be helpful in designing cities with specific LC elements arrangement that will produce a desired surface water distribution. At continental and seasonal scales, urban areas expel 12% of incoming precipitation as surface runoff during summer (JJA) as compared to 3.2% over vegetated lands, with corresponding values of 14.3% and 1.1% during winter (December–January–February). Again, this confirms that the choice of tree species in an urban setting also influences surface water discharge and may be considered to reduce the risk for flash flooding (Shepherd *et al* 2011).

Carbon sequestration caused by LC change is an important climate change issue (Milesi *et al* 2003, Nemani *et al* 2003, Bounoua *et al* 2000, 2010). We compute the carbon uptake simulated by the model for each LC class, and using the fraction of each LC within the CMG we estimate the annual carbon uptake from all classes over the continent at 7.12 PgC per year (1 PgC = 10^{15} grams of carbon), a value slightly higher than the 6.29 PgC we obtain using MODIS product, noting that MODIS carbon estimates preclude pixels labeled buildup. We compute the carbon lost due to urbanization by postulating that, under same climate, before their conversion, current urban areas had the same carbon uptake rates as surrounding vegetation they replaced. Since LC classes differ in each CMG, we estimate the carbon lost to urbanization by replacing the IS by (1) the least productive vegetation class, (2) by the most productive vegetation and (3) by the weighted average carbon uptake from all vegetation classes existing in the CMG to constrain this reconstructed 'PRE-urban' scenario between two realistic extremes. The carbon lost to urbanization is then

Table 1. Winter (DJF), summer (JJA) and annual mean precipitation and surface runoff (mm d^{-1}) for Atlanta and Washington DC averaged over the urban and the vegetation class with the highest fraction. Bold figures represent the ratio of surface runoff to precipitation in percent. MF (for Atlanta) and BD (for Washington DC) stand for mixed forest and broadleaf deciduous trees, respectively.

City			DJF mean		JJA mean		Annual mean		Actual runoff
Atlanta	Precipitation		2.71		3.52		2.85		
	Surface runoff	Urban	1.69	**62.4**	1.67	**47.0**	1.58	**55.4**	**28.9**
		MF	0.12	**4.4**	0.11	**3.1**	0.11	**3.9**	**1.6**
Washington DC	Precipitation		1.85		3.70		2.38		
	Surface runoff	Urban	0.95	**51.4**	1.67	**45.0**	1.17	**49.2**	**25.7**
		BD	0.04	**2.2**	0.57	**15.4**	0.24	**10.1**	**2.4**

obtained by subtracting the total actual carbon uptake in the CMG from that of the 'pre-urban' condition. To put the estimated carbon loss into context, we compare it to the carbon gain since pre-agriculture (Imhoff *et al* 2004) using the same methodology.

In the 'maximum impact' scenario, i.e. urbanization and croplands have both replaced the most productive lands; the carbon lost to urbanization represents 1.8% of the total continental uptake, whereas carbon gain from agriculture represents 5.0% of the total. While statistically distinct, these numbers are striking considering agriculture occupies 32.1% of the total land while urban impervious areas occupy only 1.1% over the continental US. The carbon loss is 0.9% if both agriculture and urbanization took place over the least productive lands. The carbon lost to urbanization estimated here is in agreement with previous estimates (Imhoff *et al* 2004). However, the amount of carbon uptake gained from agriculture obtained in this study (5%) is higher than that previously estimated (1.8%) using coarse resolution satellite data (DeFries *et al* 1999).

transpiration-driven cooling is a major factor modulating the SUHI, and that smaller cities, occupying about one third (35%) of their environment, may generate less heat.

We find the ratio of surface runoff of each LC class to the incoming precipitation to be useful indicator for water discharge. On an annual mean basis and considering the observed LC composition fractions in cities of the eastern US, surface runoff in dense urban cores is about 18-fold greater than that occurring on vegetated lands. At continental scale however, urban areas expel 4 times more of incoming precipitation as surface runoff during summer (JJA) as compared to vegetated lands, with an even higher multiple in winter (December–January–February).

We estimate the maximum carbon loss due to replacement of productive lands by ISs at 1.8% of the total uptake over the continental US as compared to 5.0% gain from agriculture. These carbon estimates are revealing of the significant impact of ISs on land productivity since agriculture represents 32.1% and the impervious area represents only 1.1% of the total continental US land.

4. Conclusion

Unlike previous studies providing a static remote sensing analysis of the UHI effect over the continental US; we use a fusion of Landsat and MODIS products within the SiB2 model to dynamically simulate the impact of urbanization, as a form of land use, on the surface energy, carbon and water cycles for the year 2001.

For US cities built in forested areas, the model simulated an urban LST higher than that of vegetated lands for much of the daytime. In most cases, the absolute maximum temperature difference between urban and vegetated lands is more than 3 °C. In contrast, for cities built in desert like environments such as Phoenix and similar cities, in which the urban core is greener than its surrounding due irrigated exotic vegetation, the model simulated an urban heat sink characterized by urban temperatures slightly cooler than surroundings during daytime. Averaged over CONUS, cities are warmer than vegetated lands by 1.9 °C during summer and 1.5 °C during winter. Our results strongly support the concept that

Acknowledgments

References

Akbari H 2002 Shade trees reduce building energy use and CO$_2$ emissions from power plants *Environ. Pollut.* **116** S119–26

Bounoua L, Collatz G J, Los S O, Sellers P J, Dazlich D A, Tucker C J and Randall D A 2000 Sensitivity of climate to changes in NDVI *J. Clim.* **13** 2277–92

Bounoua L, Hall F G, Sellers P J, Kumar A, Collatz G J, Tucker C J and Imhoff M L 2010 Quantifying the negative feedback of vegetation to greenhouse warming: a modeling approach *Geophys. Res. Lett.* **37** L23701

Bounoua L, Safia A, Masek J, Peters-Lidard C and Imhoff M L 2009 Impact of urban growth on surface climate: a case study in Oran, Algeria *J. Appl. Meteorol. Climatol.* **48** 217–31

Bounoua L, Zhang P, Safia A, Masek J, Imhoff M, Thome K and Wolfe R E 2015 Mapping biophysical parameters for land surface modeling over the continental US using MODIS and landsat *Dataset Pap. Sci.* **2015** 564279

Colello G D, Grivet C, Sellers P J and Berry J A 1998 Modeling of energy, water, and CO$_2$ flux in a temperate grassland

ecosystem with SiB2: May–October 1987 *J. Atmos. Sci.* **55** 1141–69

DeFries R S, Field C B, Fung I, Collatz G J and Bounoua L 1999 Combining satellite data and biogeochemical models to estimate global effects of human-induced land cover change on carbon emissions and primary productivity *Glob. Biogeochem. Cycles* **13** 803–15

Gober P, Brazel A, Quay R, Myint S, Grossman-Clarke S, Miller A and Rossi S 2009 Using watered landscapes to manipulate urban heat island effects: how much water will it take to cool phoenix? *J. Am. Plan. Assoc.* **76** 109–21

Grimmond C S B, King T S, Cropley F D, Novak D J and Souch C 2002 Local-scale fluxes of carbon dioxide in urban environments: methodological challenges and results from Chicago *Environ. Pollut.* **116** S243–54

Güneralp B and Seto K C 2013 Futures of global urban expansion: uncertainties and implications for biodiversity conservation *Environ. Res. Lett.* **8** 014025

Homer C, Huang C, Yang L, Wylie B and Coan M 2004 Development of a 2001 national land-cover database for the United States *Photogramm. Eng. Remote Sens.* **70** 829–40

Imhoff M L, Bounoua L, DeFries R, Lawrence W T, Stutzer D, Tucker C J and Ricketts T 2004 The consequences of urban land transformation on net primary productivity in the United States *Remote Sens. Environ.* **89** 434–43

Imhoff M L, Zhang P, Wolfe R E and Bounoua L 2010 Remote sensing of the urban heat island effect across biomes in the continental USA *Remote Sens. Environ.* **114** 504–13

McDonald R I *et al* 2014 Water on an urban planet: urbanization and the reach of urban water infrastructure *Glob. Environ. Change* **27** 96–105

Mahmood R *et al* 2014 Land cover changes and their biogeophysical effects on climate *Int. J. Climatol.* **34** 929–53

Milesi C, Elvidge C D, Nemani R R and Running S W 2003 Assessing the impact of urban land development on net primary productivity in the southeastern United States *Remote Sens. Environ.* **86** 401–10

Nemani R R *et al* 2003 Climate-driven increases in global terrestrial net primary production from 1982 to 1999 *Science* **300** 1560–3

Oleson K W, Monagham A, Wilhelmi O, Barlage M, Brunsell N, Feddema J, Hu L and Steinhoff, D F D F 2013 Interaction between urbanization, heat stress, and climate change *Clim. Change* **129** 525–41

Oke T R 1982 The energetic basis of the urban heat island *Q. J. R. Meteorol. Soc.* **108** 1–24

Oke T R 1988 The urban energy balance *Prog. Phys. Geogr.* **12** 471–508

Pearlmutter D, Berliner P and Shaviv E 2007 Urban climatology in arid regions: current research in the Negev desert *Int. J. Climatol.* **27** 1875–85

Quattrochi D A, Lam N S-N, Qiu H-L and Zhao W 1997 Image characterization and modeling system (ICAMS): a geographic information system for the characterization and modeling of multiscale remote sensing data *Scaling of Remote Sensing Data for GIS* ed D A Quattrochi and M F Goodchild (Boca Raton, FL: CRC Press) pp 295–307

Quattrochi D A, Estes M G Jr, Laymon C A, Crosson W L, Howell B F, Luvall J C and Rickman D L 2007 Urban heat islands. *Our Changing Planet: The View from Space* ed M D King *et al* (Cambridge: Cambridge University Press) pp 298–301

Qureshi S 2010 The fast growing megacity Karachi as a frontier of environmental challenges: Urbanization and contemporary urbanism issues *J. Geography Reg. Plan.* **3** 306–21

Ramamurthy P and Bou-Zeid E 2014 Contribution of impervious surfaces to urban evaporation *Water Resour. Res.* **50** 2889–902

Sajjad S H, Shirazi S A, Khan M A and Raza A 2009 Urbanization effects on temperature trends of Lahore during 1950–2007 *Int. J. Clim. Change Strateg. Manage.* **1** 274–81

Sellers P J *et al* 1996a A revised land surface parameterization (SiB2) for atmospheric GCMs: I. Model formulation *J. Clim.* **9** 676–705

Sellers P J *et al* 1996b A revised land surface parameterization (SiB2) for atmospheric GCMs: II.The generation of global fields of terrestrial biophysical parameters from satellite data *J. Clim.* **9** 706–37

Shepherd J M 2006 Evidence of urban-induced precipitation variability in arid climate regimes *J. Arid Environ.* **67** 607–28

Shepherd J M, Andersen T, Chris Strother A, Horst L, Bounoua and Mitra C 2013 Urban climate archipelagos: a new framework for urban impacts on climate *Earthzine*

Shepherd J M *et al* 2011 An overview of synoptic and mesoscale factors contributing to the disastrous Atlanta flood of 2009 *Bull. Am. Meteorol. Soc.* **92** 861–70

Stefanova L 2001 Sensitivity of seasonal forecast to the parameterization of land surface processes *PhD thesis* Department of Meteorology, The Florida State University p 125

Stone B Jr, Vargo J, Liu P, Hu Y and Russell A 2013 Climate change adaptation through Urban heat management in Atlanta, Georgia *Environ. Sci. Technol.* **47** 7780–6

Tan B, Morisette J T, Wolfe R E, Gao F, Ederer G A, Nightingale J and Pedelty J A 2011 An enhanced TIMESAT algorithm for estimating vegetation phenology metrics from MODIS data *IEEE J. Sel. Top. Earth Obs. Remote Sens.* **4** 361–71

UNFPA (United Nations Population Fund) 2007 *State of World Population. Unleashing the Potential of Urban Growth* (www.unfpa.org/swp/2007/english/introduction.html, accessed 21 February 2015)

Voogt J A and Oke T R 2003 Thermal remote sensing of urban climates *Remote Sens. Environ.* **86** 370–84

Walker J J, de Beurs K M and Henebry G M 2015 Land surface phenology along urban to rural gradients in the US great plains *Remote Sens. Environ.* **165** 42–52

Zhang P, Imhoff M, Wolfe R and Bounoua L 2010 Characterizing urban heat islands of global settlements using MODIS and nighttime lights products *Can. J. Remote Sens.* **36** 185–96

Zhang P, Imhoff M, Bounoua L and Wolfe R 2012 Exploring the influence of impervious surface density and shape on urban heat islands in the northeast United States using MODIS and Landsat *Can. J. Remote Sensing* **38** 441–51

Zhao L, Xuhui L, Smith R B and Oleson K 2014 Strong contributions of local background climate to urban heat islands *Nature* **511** 216–9